Efficient Polymer Solar Cells with a High Open Circuit Voltage of 1 Volt

*Jianyu Yuan, Zhichun Zhai, Huilong Dong, Jing Li, Zuoquan Jiang, Youyong Li, and Wanli Ma**

A series of polymers containing benzo[1,2-b:4,5-b′]dithiophene and N-alkylthieno[3,4-c]pyrrole-4,6-dione are designed. By incorporating different alkylthienyl side chains, the fill factor (FF) and open circuit voltage (V_{oc}) of the copolymers are further improved. The experimental results and theoretical calculations show that the size and topology of the side chains can influence the polymer solubility, energy levels, and intermolecular packing by altering the molecular coplanarity. As a result of improved morphology and fine-tuned energy levels, an increased FF and a high V_{oc} of 1.00 V are achieved, as well as a power conversion efficiency of 6.17%, which is the highest efficiency ever reported for polymer solar cells with a V_{oc} over 1 V.

1. Introduction

Research on polymer solar cells (PSCs) has attracted tremendous scientific and industrial interest in recent years.[1] One major obstacle to a large scale commercialization of PSCs is the relatively low device efficiencies. The best power conversion efficiencies (PCEs) for small-area devices have been in the range of 5–6% for many years.[2] In the last several years, however, there has been exciting progress in the synthesis of novel low-bandgap polymers by using the donor-acceptor copolymerization.[3] Based on these polymers, PCEs over 7% have been widely reported.[3a,4] Nevertheless, the further improvement of device efficiency by using new materials has been extremely difficult due to the difficulties in polymer synthesis and the inherent disadvantages of organic materials, such as limited absorption range and relatively low carrier mobility.

The adoption of new device architectures, such as tandem structure has been demonstrated to be a simple approach to further improve device performance. Very recently, Yang et al. reported a PCE of 8.62% using tandem structure, which is the highest certified efficiency for PSCs to date.[5] An efficiency of 10.7% was achieved by the company Heliatek for small molecule tandem solar cells.[6] A typical polymer tandem structure consists of a front cell using a large-bandgap material and a rear cell comprising a low-bandgap material. So far most materials for tandem cells have focused on low-bandgap polymers aiming to achieve high short circuit current density (J_{sc}). There have been very few reports of large-bandgap polymers designed specifically to improve open circuit voltage (V_{oc}) for high-efficiency tandem PSCs. Poly(3-hexylthiophene) (P3HT) has been used as the large-bandgap material in most tandem PSCs,[7] although it suffers from a low V_{oc} of only 0.6 V due to its shallow HOMO (highest occupied molecular orbital) energy level. The performance of current tandem PSCs can be significantly improved if P3HT is replaced by an efficient large-bandgap polymer which has a deeper HOMO and hence a significant larger V_{oc}. Nonetheless, to the best of our knowledge, single junction polymer solar cells that have PCEs over 5% while maintaining a V_{oc} of 1 V have not been reported. Recently, a series of D-A copolymers using benzo[1,2-b:4,5-b′]dithiophene (BDT) as the donor comonomer and N-alkylthieno[3,4-c]pyrrole-4,6-dione (TPD) as the acceptor comonomer have been synthesized by four research groups at almost the same time.[8] These copolymers have a great potential as the large-bandgap materials in tandem PSCs because they simultaneously demonstrate both a good efficiency of 4–6% and a large V_{oc} of 0.8–0.9 V. In this study, our goal is to fine-tune the energy levels of these copolymers to design them specifically for tandem cells. Herein, we report a further improvement of their fill factor (FF), V_{oc}, and PCE by incorporating three different alkylthienyl side chains to the BDT unit to replace the original alkoxy side chains. The introduction of conjugated thienyl side chains enhances the coplanarity of the polymer and may consequently lead to a broader absorption, higher charge mobilities and deeper HOMO, thereby resulting in improved FF and PCEs.[4d,9] The size and topology (e.g., linear, branched) of the alkyl side chains appended to the thiophone moiety could also affect the coplanarity, morphology, and photovoltaic parameters (J_{sc}, V_{oc}, and FF) of the materials.[10] With optimal side chains, the tailored polymer demonstrated an increased FF, a high V_{oc} of 1.00 V and a PCE of 6.17%, which is the highest efficiency ever reported for polymers with a V_{oc} over 1 V. The new copolymer has a similar bandgap to P3HT but shows a significantly improved V_{oc} and PCE, making it a better candidate than P3HT for use as a large-bandgap material in tandem solar cells.

J. Yuan, Z. Zhai, H. Dong, J. Li, Z. Jiang, Prof. Y. Li, Prof. W. Ma
Institute of Functional Nano & Soft Materials (FUNSOM)
Soochow University
199 Ren-Ai Road, Suzhou Industrial Park, Suzhou, Jiangsu 215123, China
E-mail: wlma@suda.edu.cn

DOI: 10.1002/adfm.201201535

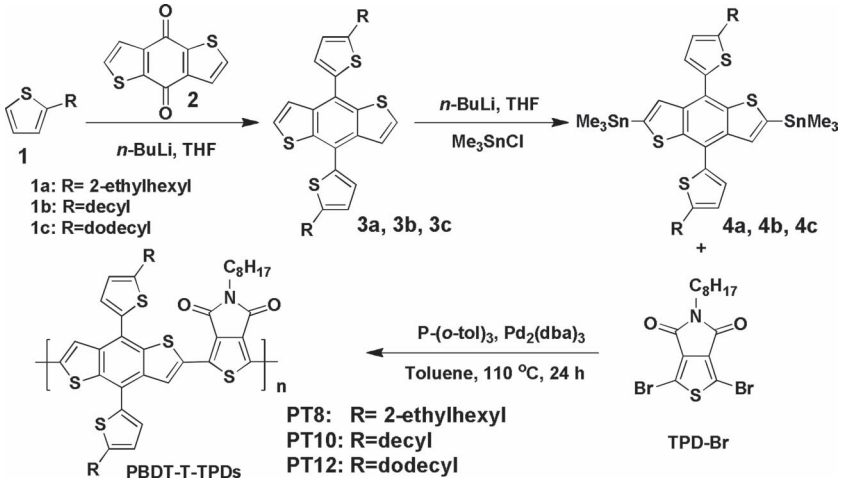

Scheme 1. Synthesis of PBDT-T-TPDs.

2. Results and Discussion

2.1. Synthesis of Monomers and Polymers

The preparation of PBDT-T-TPDs is detailed in **Scheme 1**. A Stille cross-coupling reaction was used between bis(trimethyl stannane) of BDT-T and dibromides of TPD. The synthesis is simple and results in high yields. The precursors of TPD-Br monomers can be prepared through a four-step procedure starting from thiophene-3,4-dicarboxylic acid.[8] The polymerization reactions for polymers with different side-chains were carried out under almost the same conditions and all of them gave high yields (≈85%). The three polymers exhibit good solubility in commonly used solvents such as tetrahydrofuran (THF), chloroform (CF), and chlorobenzene (CB). Among them, PT8 shows the best solubility due to its branched alkyl side chains. Molecular weight of the polymers and polydispersity (PDI) was estimated by gel permeation chromatography (GPC) using monodispersed polystyrene as the standard and THF as the eluent (**Table 1**). The number-average molecular weight (M_n) of PT8, PT10, and PT12 are 37 200, 36 800, and 49 900 g/mol, respectively.

2.2. Thermal and Optical Properties

Thermal stability of three polymers was investigated by thermogravimetric analysis (TGA). As shown in **Figure 1** and Table 1, all the copolymers show good thermal stability under nitrogen atmosphere with the 5% weight-loss temperature (T_d) at 423, 442, and 432 °C for PT8, PT10, and PT12, respectively. The excellent thermal stability is consistent with the previous reports that the incorporation of alkylthienyl side chains is helpful to improve polymer thermal stability.[4d,9b] Since all three polymers have similar T_d, we conclude that the size and topology of the alkyl side chains attached to the thienyl moiety do not play a critical role in determining the polymer thermal stability.

UV-vis absorption spectra of PBDT-T-TPDs are shown in **Figure 2**. The polymer solutions in chloroform display a board absorption from 400 to 680 nm. For polymers with linear alkyl side chains, both PT10 and PT12 show a distinct shoulder peak next to the absorption maximum in their solution and solid state spectra, which is typical for BDT based copolymers.[11] We noticed that the absorption peaks of the two polymers are almost the same, indicating that the length of the linear side chains has only a slight effect on the polymer bandgap. No red-shift is observed between their absorption spectra in solution and solid state. It is speculated that a certain degree of packing was formed even in the diluted solution, likely due to limited solubility.[8a,c,12] For the polymer with branched alkyl side chains, PT8 shows an apparently less broad absorption spectrum in CF and the absorption maximum is blue shifted. The introduction of bulkier side chains therefore increases the polymer bandgap and reduces the packing in solution, likely due to enhanced solubility. From the onset of the film absorption spectra, optical bandgap values of about ≈1.8–1.9 eV were estimated for the three polymers.

Table 1. Molecular weights and thermal properties of the polymers.

Polymer	M_n [g/mol][a)]	M_w [g/mol][a)]	PDI[a)]	T_d [°C][b)]	Solubility [g/L][c)]
PBDT-T8-TPD	37 200	79 800	2.14	423	16
PBDT-T10-TPD	36 800	66 500	1.81	442	10
PBDT-T12-TPD	49 900	78 500	1.57	432	11

[a)]Termined by GPC using polystyrene standards and THF as eluent; [b)]Percentage weight loss temperatures measured by TGA under nitrogen atmosphere; [c)]The concentration of its saturated solution in chloroform at 25 °C.

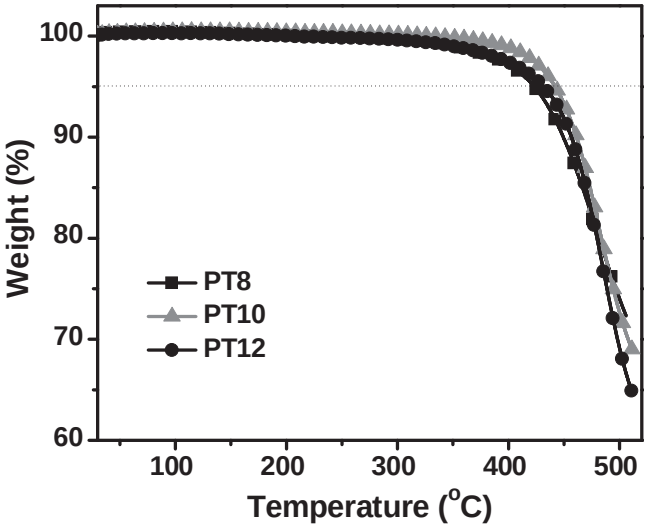

Figure 1. TGA curves of PBDT-T-TBDs with a heating rate of 10 °C/min under an inert atmosphere.

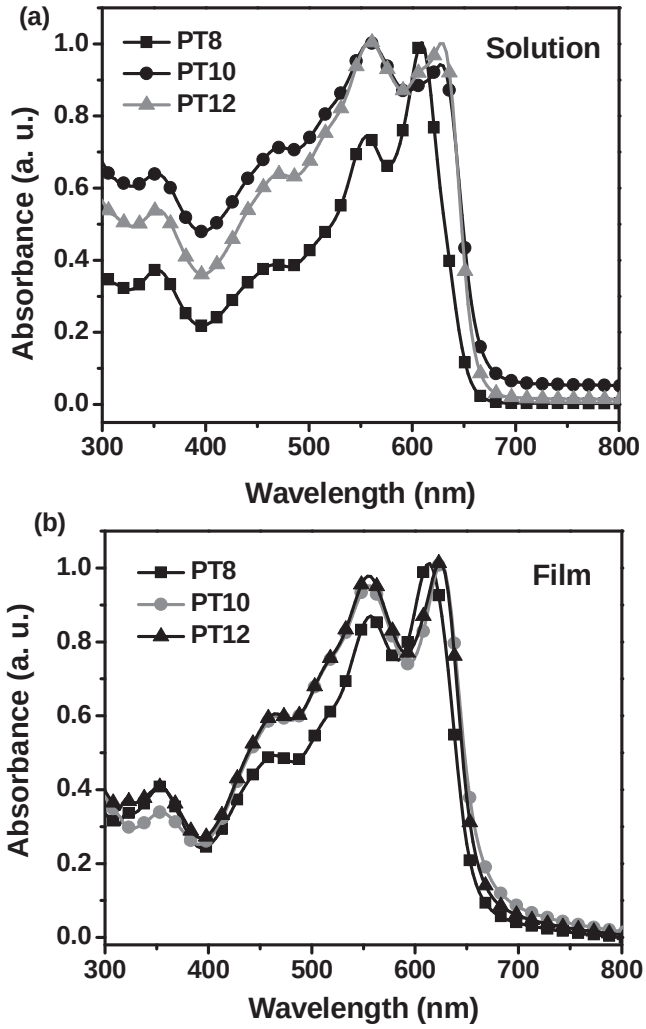

Figure 2. Normalized UV-vis absorption spectra of PBDT-T-TPDs in dilute chloroform solution (a) and a thin film spin-cast from chloroform (b).

2.3. Electrochemical Properties

The polymer solutions in chloroform were coated on the platinum plate working electrode to form a thin film for a cyclic voltammetry (CV) measurements (see the Supporting Information). The highest occupied molecular orbital (HOMO) and the lowest unoccupied molecular orbital (LUMO) energy levels were calculated from the onset potential of the first oxidation and reduction peaks, respectively (**Table 2**). The polymer structure and corresponding energy levels are shown in **Scheme 2**. The bandgap measured from CV is slightly larger than that obtained from the absorption spectrum, which has been reported in previous works for other BDT-based polymers.[8a,11c] From the CV measurement results, we concluded that polymer shows a larger bandgap and a deeper HOMO energy level when incorporating bulkier side chains, with a bulkiness sequence of 2-ethylhexyl > dodecyl > decyl. We hypothesize that the steric hindrance introduced by side chains could lead to twisted polymer backbones and altered conjugation lengths, resulting in the modification of energy levels. This hypothesis will be further examined by theoretical calculations discussed below. In general, all three polymers exhibit extremely deep HOMO energy levels (below –5.50 eV), which implies that these polymers could be very stable against oxidization, hence leading to high device stability. Furthermore, such deep HOMO energy levels can result in high a V_{oc} and efficiency.

2.4. Theoretical Calculations

In order to clarify the correlation between the change in energy levels and the type of side chains, we performed density functional theory (DFT) calculations for the three monomers (T8, T10, and T12) by using the DMol3[13] program. For geometry optimizations, the generalized gradient approximation (GGA)[14] proposed by Becke, Lee, Yang and Parr,[14] along with a double numerical plus polarization (DNP) basis set, were used in molecular orbital energy level calculations. Solvent (chloroform) effects was taken into consideration by using a proper dielectric constant of 4.806.

Our calculations indicate that the HOMO energy levels are deeper and the bandgaps are larger as the number of carbons in the side chain increase for the linear-chain structured T10 and T12 (See the Supporting Information). The HOMO energy level of T8 with a branched side chain is significantly deeper than T10 and T12. These calculation results are in accordance with the relevant experimental results.

Dihedral angles between BDT and the thiophene rings of three structures were measured to compare the distortions. As seen in **Figure 3**e, the dihedral angles of T8 (48.122° and 52.683°) are relatively large and those of T10 (47.971° and 48.314°) are the smallest. For the dihedral angles between BDT and TPD, we obtain –32.284°, –17.470°, and –24.095° for T8,

Table 2. Optical and electrochemical properties of PBDT-T-TPDs.

Polymer	λ_{max} [nm] Solution	Film	λ_{onset} [nm] Solution	Film	E_g^{opt} [eV][a)]	LUMO [eV][b)]	HOMO [eV][b)]	E_g^{EC} [eV][c)]
PBDT-T8-TPD	555 609	557, 614	660	672	1.85	–3.56	–5.61	2.05
PBDT-T10-TPD	558, 627	558, 627	673	690	1.80	–3.55	–5.47	1.92
PBDT-T12-TPD	558, 627	558, 627	675	680	1.82	–3.58	–5.56	1.98

[a)] E_g^{opt} were estimated from the onset of UV-vis spectra in solutions; [b)]HOMO and LUMO levels were estimated from the onset of the oxidation and reduction peaks of cyclic voltammetry, respectively; [c)]Determined from cyclic voltammetry.

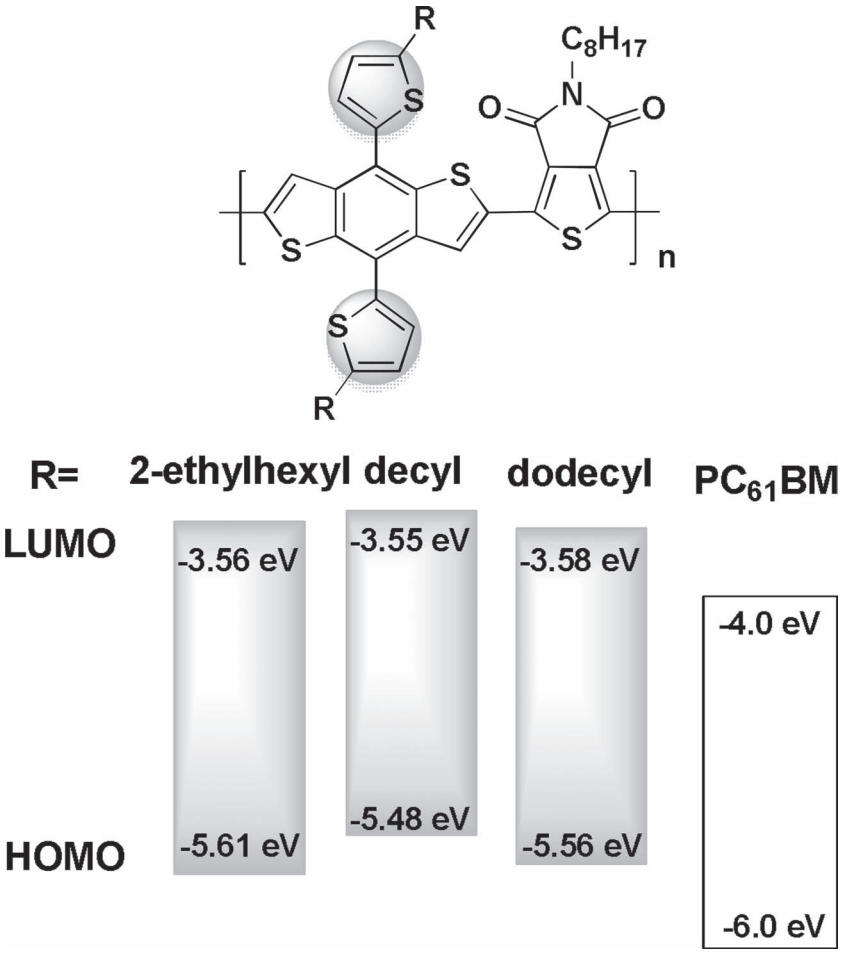

Scheme 2. Structure and energy levels of PBDT-T-TPDs and $PC_{61}BM$.

T10, and T12 respectively. These results demonstrate that the T8 structure is the most twisted, whereas the T10 structure is the most planar.

Meanwhile, molecular mechanics simulations by Forcite were carried out to compare the structural geometry of the polymers. We choose $n = 5$ to stand for the polymers, and the structures were constructed based on atactic polymerization. The Dreiding forcefield[16] was used for the calculations. The optimized structures of PT8, PT10, and PT12 show different planarity, which affect their HOMO and LUMO energies differently. To quantify the planarity of each molecule, we aligned the backbone of the molecules to XZ plane to minimize the summation of Y coordinates of each atom. The calculated standard deviations of Y coordinates of each atom (defined as Y_StDev) for PT8, PT12, and PT10 are 1.463, 1.181, and 0.695 Å, respectively (Figure 3a–d). We can see that PT10 shows the best planarity and PT8 shows the worst planarity. In general, polymer coplanarity is directly related to the size and topology of the side chains. The polymer coplanarity can not only affect the conjugation length, therefore modifying the bandgap, but also affect the molecular packing, active layer morphology and charge mobility. We further examined the effect of polymer coplanarity on charge transport by measuring their hole mobility via the space charge limited current (SCLC) method, as shown in Figure S8 and Table S2 in the Supporting Information. The hole mobilities of T8, T12, and T10 pure film are 5.9×10^{-5}, 7.0×10^{-5}, and 7.9×10^{-5} cm^2 V^{-1} s^{-1}, respectively. These results indicate that higher polymer coplanarity is beneficial for charge transport.

2.5. Photovoltaic Performance and Film Morphology

Bulk hetero-junction PSCs were fabricated using PBDT-T-TPDs and $PC_{61}BM$. The device structure is ITO/PEDOT-PSS(45 nm)/PBDT-T-TPDs:$PC_{61}BM$/LiF(1 nm)/Al(100 nm) and the device active area is 7.25 mm^2. The device optimization includes fine adjustment of solvents, additives, material concentrations and ratios. First, the choice of solvents is critical to the device performance since these polymers exhibit different solubility in various solvents. PT8 shows excellent solubility in all the solvents, including CF, CB, and *o*-dichlorobenzene (ODCB), due to its bulky side chains and twisted backbone, whereas PT10 and PT12 can be dissolved well in CF but show decreased solubility in CB and ODCB. The solubility data of three polymers are included in Table 1. Devices using different solvents were fabricated and compared, as shown in Table 3 and Table S1 (Supporting Information). The results demonstrated that the best processing condition is using CF as the solvent with a polymer concentration of 8 mg/mL and a polymer:fullerene weight ratio of 1:1. Solvent additives and mixed solvents have also been investigated to further enhance device performance. In our previous work,[2e,17] 1,8-diiodooctane (DIO) has been proven to be an efficient and universal additive to improve the morphology of polymer films. Herein, we introduced an optimal amount of DIO and enhanced device performance were observed. Mixed solvents using CB and ODCB could also lead to better PCEs, but are less efficient than using DIO.

By carefully analyzing the device photovoltaic parameters, we can elucidate the correlation between the side chains and device performance. **Table 3** and **Figure 4** show the device performance data and the current density-voltage curves (J–V curves) of the PSCs under illumination (AM1.5G 100 mW/cm^2). The three polymers cast from CF without any additives show a PCE of 2.16%, 3.14%, and 4.15% for PT8, PT12, and PT10, respectively, which is in accordance with their backbone coplanarity. The polymer coplanarity is considered to be crucial to the carrier transport and has a direct impact on the device photovoltaic parameters, such as FF and J_{sc}. Indeed, our experiments results show that PT8 has the lowest FF, J_{sc}, and PCE, whereas PT10 has the highest. However, device performance dramatically changed after the addition of DIO. We obtained a PCE of 6.17%, 4.50%, 4.51% for polymer PT8, PT12, and PT10, respectively. The change of PCEs is mainly due to the improved FF and

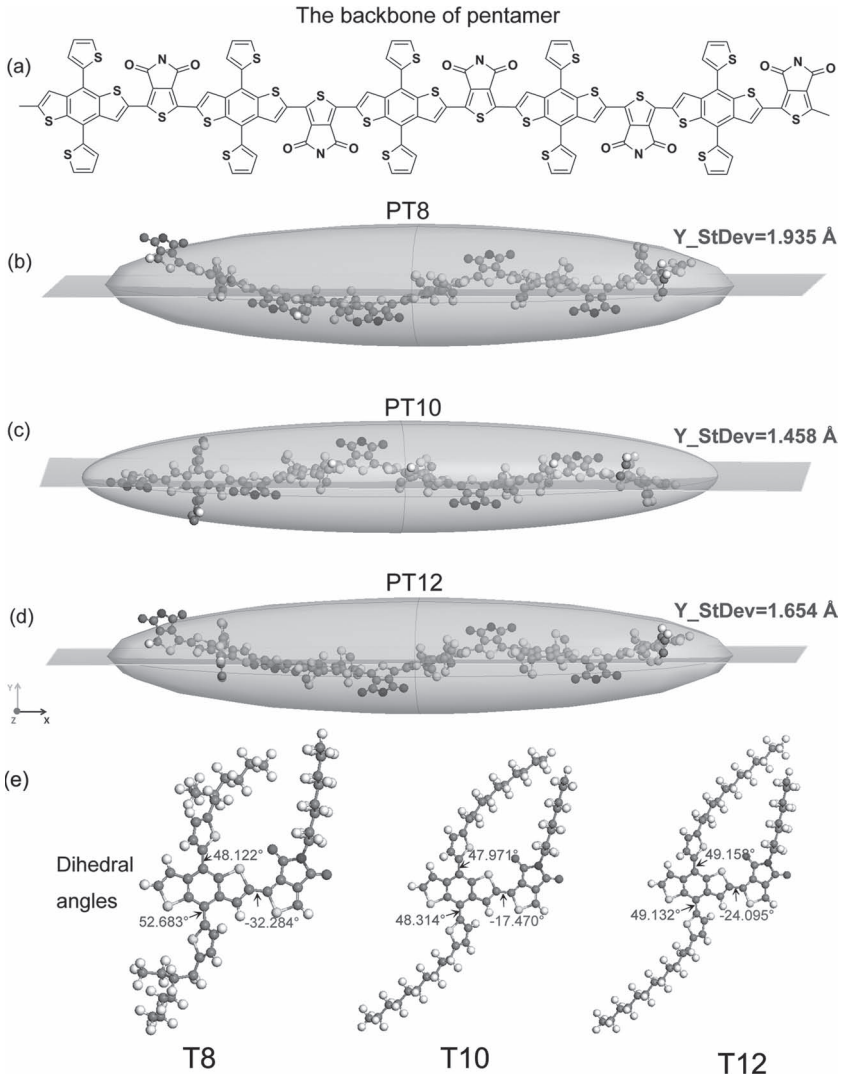

Figure 3. a) Schematic backbone structure of the pentamers. The side chains are removed for clarity. b–d) The calculated steric arrengement of backbones for PT8, PT10, and PT12, respectively. The green ellipsoids present the approximate shape of the pentamers, and the orange planes are the XZ plane. e) Several key dihedral angles of the polymer obtained from DFT calculations.

J_{sc}. Specifically, PT8 demonstrated a greatly increased FF (from 38.1% to 63.0%) and J_{sc} (from 5.90 to 9.79 mA/cm^2); PT12 showed a moderate improvement in FF (from 49.0% to 53.2%) and J_{sc} (from 6.69 to 8.94 mA/cm^2); PT10 exhibited only a slight change in FF (from 55.1% to 55.0%) and J_{sc} (from 8.18 to 8.92 mA/cm^2). The performance enhancement for PT8 is typically observed for PSCs using solvent additives which are believed to improve the polymer-fullerene phase separation and increase intermolecular packing. For PT12 and PT10, the improvement of photovoltaic performance is less pronounced, indicating that the morphology change induced by DIO is not as apparent as that of PT8. An explanation is that partially due to the limited solubility, PT12 and PT10 do not adapt the regular coil-like structure in solution, but adopt a similar rigid-rod conformation as in film, which can be proved by the zero red-shift of their film absorption spectra. Very likely, well-packed aggregates have already formed in solution state. Hence, the reorganization of the intermolecular packing and the formation of proper phase separation in the film, assisted by DIO, is less efficient than that of PT8.

In **Figure 5**, we also compared the device performance of PT8 to the original polymer PBDT-TPD (synthesized according to a previous report)[8d] which has alkoxy side chains appended to the BDT unit. We obtained a maximum PCE of 4.77% for the original polymer with a J_{sc} of 10.74 mA/cm^2, a V_{oc} of 0.90 V, and a FF of 49.4%. By replacing the alkoxy side chains with alkylthienyl side chains, T8 achieved a higher V_{oc} of 1.00 V and a FF of 63.0%. We attribute the increased V_{oc} to the fine-tuned HOMO energy level.

Table 3. Photovoltaic properties of PSCs based on PBDT-T-TPDs and PBDT-TPD, under the illumination of AM1.5G, 100 mW/cm^2.

Polymer	Solvent	J_{sc} [mA/cm^2]	V_{oc} [V]	FF [%]	PCE [%]
PBDT-T8-TPD	CF	5.90	0.96	38.1	2.16
PBDT-T8-TPD	CF+3%DIO	9.79	1.00	63.0	6.17
PBDT-T10-TPD	CF	8.18	0.92	55.1	4.15
PBDT-T10-TPD	CF+3%DIO	8.92	0.92	55.0	4.51
PBDT-T12-TPD	CF	6.69	0.96	49.0	3.14
PBDT-T12-TPD	CF+3%DIO	8.94	0.95	53.2	4.50
PBDT-TPD	CF	8.63	0.85	47.5	3.48
PBDT-TPD	CF+2% DIO	10.74	0.90	49.4	4.77

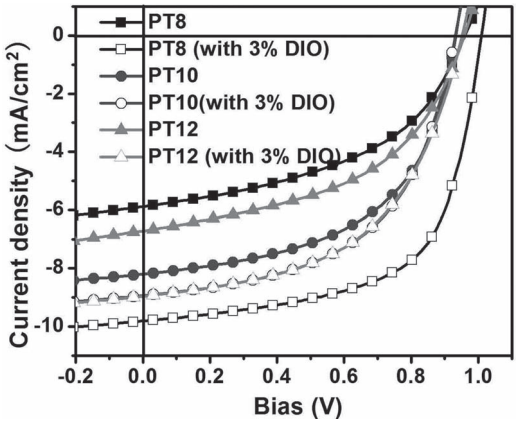

Figure 4. Current density-voltage characteristics of ITO/PEDOT:PSS/PBDT-T-TPDs:$PC_{61}BM$/LiF/Al devices spin-cast from chloroform (W/O DIO) under illumination of AM 1.5 G at 100 mW/cm^2.

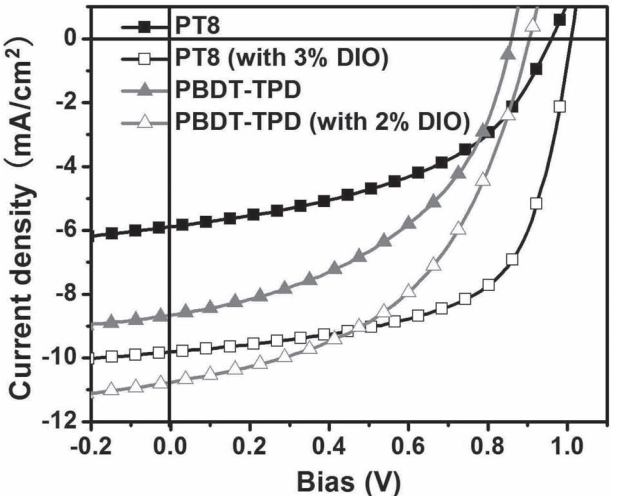

Figure 5. Current density-voltage characteristics of the PSCs based on PT8 and PBDT-TPD spin-cast from chloroform (W/O DIO) under illumination of AM 1.5 G at 100 mW/cm^2.

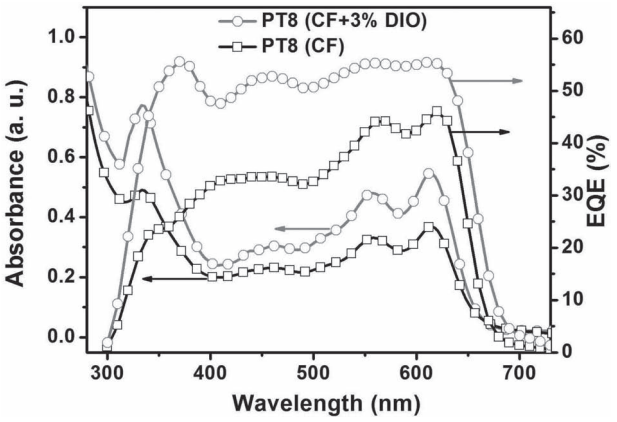

Figure 6. Absorption and EQE spectra of PBDT-T8-TPD/$PC_{61}BM$ (1:1 weight ratio) blends cast from chloroform or chloroform with 3% DIO.

The enhanced FF is very likely due to the improved intermolecular packing assisted by the thienyl side groups. To evaluate the photoresponse of PT8 and calibrate the J_{sc} data, external quantum efficiencies (EQE) of the devices with or without DIO were measured (**Figure 6**). The device showed a relatively high photo-conversion efficiency over the whole wavelength range of 380–670 nm, with monochromatic EQE values around 50–60%. The J_{sc} calculated by integrating the EQE curve with an AM1.5G reference spectrum is within 5% error compared to the corresponding J_{sc} obtained from the J–V curves.

The effects of polymer solubility and solvent additive on film morphology were investigated by using atomic force microscopy (AFM) and transmission electron microscopy (TEM). AFM height (**Figure 7**) and phase images (Figure S7, Supporting Information) were measured on film cast from the polymer/$PC_{61}BM$ blend with or without DIO. The film surface roughness without DIO is 0.81, 1.46, and 2.01 nm for PT8, PT12, and PT10 respectively. We noticed that the polymer with less bulky side chains showed a larger surface roughness and domain size, likely due to the decreased solubility. DIO is believed to allow a slower crystallization process during spin-coating, thus improving morphology through enhanced intermolecular ordering and well-developed phase separation.[18] Therefore, we observed that PT8 processed with DIO exhibited fine phase separation domains, leading to a more efficient charge transport. For PT10, the addition of DIO further enhanced the phase segregation, leading to an unfavorable large domain size for charge dissociation and transport. In order to confirm the speculation, we also investigated the film morphology by using TEM, as shown in **Figure 8**. For PT8, after the addition of DIO, the morphology showed a dramatic change from the original smooth film to a network structured film with interconnected polymer nanofibers, which is the desired morphology for efficient carrier transport. However, for PT10, distinctive phase separation has already been established. The addition of DIO did not make a significant change to the film morphology. Compared to PT8 processed with DIO, the nanofibers in the film of PT10 are not as well interconnected.

3. Conclusions

In order to specifically design a large-bandgap polymer for tandem PSCs, we have successfully modified a series of polymers containing a BDT-TPD backbone by the incorporation of different alkylthienyl side chains, aiming to further improve the V_{oc} and FF of the copolymers. Both experimental results and theoretical calculations have shown that the size and topology of the alkyl chains can fine-tune the polymer solubility, energy levels, and intermolecular packing by altering the molecular coplanarity. The polymer solubility, coplanarity and the use of additives play critical roles in improving the morphology of the polymer-fullerene blend. By using only commercially available $PC_{61}BM$ instead of expensive $PC_{71}BM$ or specially synthesized fullerene derivatives, the optimized solar cells demonstrated an increased FF, a high V_{oc} of 1.00 V, and a PCE above 6.17%, which is the highest efficiency ever reported for PSCs with a V_{oc} over 1 V. The new copolymer has a similar bandgap to P3HT

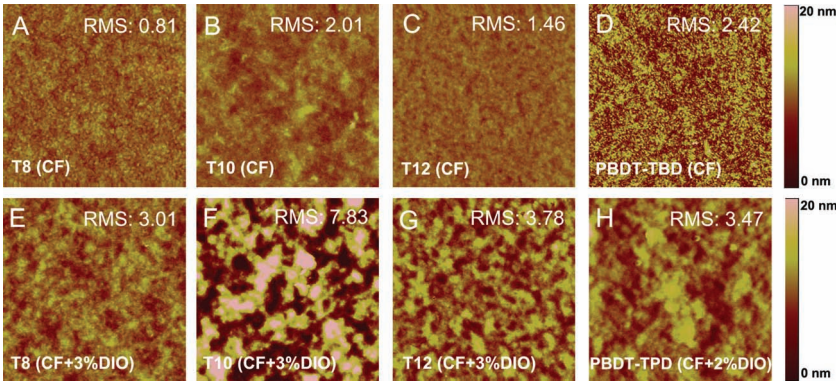

Figure 7. a–h) AFM height images (5.0 μm × 5.0 μm) of polymer/$PC_{61}BM$ (1:1 weight ratio) blends cast from chloroform or chloroform with DIO.

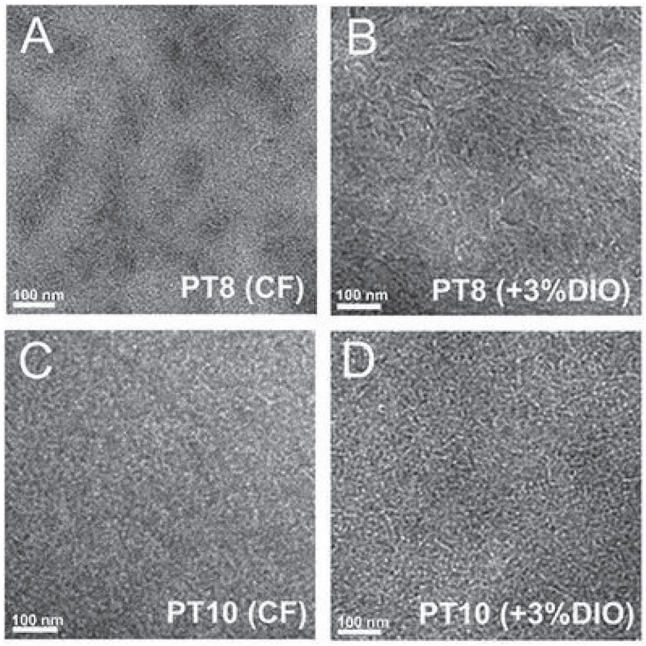

Figure 8. TEM images of polymer/$PC_{61}BM$ blends (1:1 weight ratio) cast from chloroform or chloroform with 3% DIO.

but shows a significantly improved V_{oc} and PCE, which makes it a better candidate than P3HT for the large-bandgap material used in tandem PSCs.

4. Experimental Section

Characterization: UV-vis-NIR spectra were recorded on a Perkin Elmer model Lambda 750. Thermogravimetric analysis (TGA) was carried out using a Perkin Elmer TGA4000 instrument. Atomic force microscopy (AFM) and transmission electron microscopy (TEM) images were obtained using a Veeco Multimode V instrument and Tecnai G2 F20 S-Twin transmission electron microscope, respectively.

Synthesis of PBDT-T-TPDs: In a 50 mL reaction tube, compound 4a–4c (0.3 mmol), TPD-Br (0.13 g, 0.3 mmol) tri(*o*-tolyl)phosphine (0.02 g, 0.08 mmol), and $Pd_2(dba)_3$ (0.01 g, 0.01 mmol) were dissolved in 5 mL dry toluene under argon. After stirring at 110 °C for 24 h, the mixture was cooled to room temperatures and precipitated in methanol (130 mL). The precipitate was filtered and washed with methanol (24 h) and hexane (24 h) successively in a Soxhlet apparatus to remove oligomers and catalyst residue. Finally, the polymer was extracted with chloroform (10 h). The chloroform fraction was concentrated and precipitated in methanol. The precipitate was filtered and dried in vacuum at 80 °C overnight. PBDT-T8-TPD: obtain as dark purple solid (231 mg, 85%), GPC: M_n = 37 200 g mol^{-1}, PDI = 2.14. ^{1}H NMR (400 MHz, $CDCl_3$, δ): 9.12-8.00 (br, 4H ArH), 7.26-6.50 (br, 2H ArH), 3.30-3.98 (br, 2H NCH_2), 2.61-3.30 (br, 4H), 2.20-1.20 (br, 30H), 1.20-0.80 (br, 15H). PBDT-T10-TPD: obtain as dark purple solid (237 mg, 86%), GPC: M_n = 36 800 g mol^{-1}, PDI = 1.81. ^{1}H NMR (400 MHz, $CDCl_3$, δ): 9.12-8.00 (br, 4H ArH), 7.26-6.50 (br, 2H ArH), 3.30-3.98 (br, 2H NCH_2), 2.61-3.30 (br, 4H), 2.25-1.20 (br, 38H). 1.20-0.75 (br, 15H). PBDT-T12-TPD: obtain as dark purple solid (250 mg, 83%), GPC: M_n = 49 900 g mol^{-1}, PDI = 1.57. ^{1}H NMR (400 MHz, $CDCl_3$, δ): δ (ppm) 9.12-8.00 (br, 4H ArH), 7.26-6.50 (br, 2H ArH), 3.30-3.98 (br, 2H NCH_2), 2.61-3.30 (br, 4H), 2.50-1.20 (br, 46H), 1.20-0.75 (br, 15H).

Device Fabrication and Testing: Polymer solar cells were fabricated with a general structure of ITO/PEDOT-PSS (45 nm)/polymer:PCBM/LiF/Al. Patterned ITO glass substrates were cleaned by sequential ultrasonic treatment in detergent, acetone, deionized water and isopropyl alcohol. The organic residue was further removed by treating with UV-ozone for 10 min. A thin film of PEDOT: PSS (≈45 nm) was spin-coated on ITO substrates and dried at 150 °C for 10 min. A blend of PBDT-T-TPDs and PCBM with different ratios was dissolved in chloroform or chlorobenzene containing 0–5% (v/v) diiodooctane, filtered through a 0.45 μm poly(tetrafluoroethylene) (PTFE) filter, spin-coated at 1000 rpm for 60 s, 1.0 nm of LiF (0.2A/s) and 100 nm Al (2A/s) layers were then thermally evaporated on the active layer at a pressure of 1.0×10^{-6} mbar through a shadow mask (active area 7.25 mm^2). The current density-voltage characteristics of the photovoltaic cells were measured using a Kheithey 2400 (*I–V*) digital source meter under simulated AM 1.5G solar irradiation at 100 mW/cm^2 (Newport, Class AAA solar simulator, 94023A-U). The light intensity was calibrated by a certified Oriel Reference Cell (91150V) and verified with a NREL calibrated Hamamatsu S1787-04 diode. The external quantum efficiency (EQE) was performed using a certified IPCE instrument (Zolix Instruments, Inc, SolarCellScan100).

Supporting Information

Supporting Information is available from the Wiley Online Library or from the author.

Acknowledgements

This work was supported by the National High Technology Research and Development Program of China (863 Program) (grant no. 2011AA050520), the National Natural Science Foundation of China (grant no. 61176054), the Priority Academic Program Development of Jiangsu Higher Education Institutions.

Received: June 8, 2012
Revised: July 23, 2012
Published online: September 17, 2012

[1] a) G. Yu, J. Gao, J. C. Hummelen, F. Wudl, A. J. Heeger, *Science* **1995**, *270*, 1789; b) S. Gunes, H. Neugebauer, N. S. Sariciftci, *Chem. Rev.* **2007**, *107*, 1324; c) B. C. Thompson, J. M. J. Fréchet, *Angew. Chem. Int. Ed.* **2008**, *47*, 58; d) G. Dennler, M. C. Scharber, C. J. Brabec, *Adv. Mater.* **2009**, *21*, 1323; e) Y.-J. Cheng, S.-H. Yang, C.-S. Hsu, *Chem. Rev.* **2009**, *109*, 5868.

[2] a) W. Ma, C. Y. Yang, X. Gong, K. Lee, A. J. Heeger, *Adv. Funct. Mater.* **2005**, *15*, 1617; b) G. Li, V. Shrotriya, J. S. Huang, Y. Yao, T. Moriarty, K. Emery, Y. Yang, *Nat. Mater.* **2005**, *4*, 864; c) W. L. Wang, H. B. Wu, C. Y. Yang, C. Luo, Y. Zhang, J. W. Chen, Y. Cao, *Appl. Phys. Lett.* **2007**, *90*, 183512; e) J. Peet, J. Y. Kim, N. E. Coates, W. L. Ma, D. Moses, A. J. Heeger, G. C. Bazan. *Nat. Mater.* **2007**, *6*, 497.

[3] a) H.-Y. Chen, J. H. Hou, S. Q. Zhang, Y. Y. Liang, G. W. Yang, Y. Yang, L. P. Yu, Y. Wu, G. Li, *Nat. Photonics* **2009**, *3*, 649; b) Y. Liang, Z. Xu, J. Xia, S.-T. Tsai, Y. Wu, G. Li, C. Ray, L. Yu, *Adv. Mater.* **2010**, *22*, E135; c) H. Zhou, L. Yang, A. C. Stuart, S. C. Price, S. Liu, W. You, *Angew. Chem. Int. Ed.* **2011**, *50*, 2995; d) H. J. Son, W. Wang, T. Xu, Y. Liang, Y. Wu, G. Li, L. Yu, *J. Am. Chem. Soc.* **2011**, *133*, 1885; e) Z. He, C. Zhong, X. Huang, W.-Y. Wong, H. Wu, L. Chen, S. Su, Y. Cao, *Adv. Mater.* **2011**, *23*, 4636.

[4] a) C. M. Amb, S. Chen, K. R. Graham, J. Subbiah, C. E. Small, F. So, J. R. Reynolds, *J. Am. Chem. Soc.* **2011**, *133*, 10062; b) S. C. Price, A. C. Stuart, L. Yang, H. Zhou, W. You, *J. Am. Chem. Soc.* **2011**,

133, 4625; c) T.-Y. Chu, J. Lu, S. Beaupré, Y. Zhang, J.-R. m. Pouliot, S. Wakim, J. Zhou, M. Leclerc, Z. Li, J. Ding, Y. Tao, *J. Am. Chem. Soc.* **2011**, *133*, 4250; d) L. J. Huo, S. Q. Zhang, X. Guo, F. Xu, Y. F. Li, J. H. Hou, *Angew. Chem. Int. Ed.* **2011**, *50*, 9697.

[5] L. Dou, J. You, J. Yang, C.-C. Chen, Y. He, S. Murase, T. Moriarty, K. Emery, G. Li, Y. Yang, *Nat. Photonics* **2012**, *6*, 180.

[6] http://www.heliatek.com/(last accessed September 2012).

[7] a) J. Y. Kim, K. Lee, N. E. Coates, D. Moses, T.-Q. Nguyen, M. Dante, A. J. Heeger, *Science* **2007**, *317*, 222; b) S. Sista, Z. Hong, M.-H. Park, Z. Xu, Y. Yang, *Adv. Mater.* **2010**, *22*, E77; c) S. Sista, M.-H. Park, Z. Hong, Y. Wu, J. Hou, W. L. Kwan, G. Li, Y. Yang, *Adv. Mater.* **2010**, *22*, 380.

[8] a) Y. Zhang, S. K. Hau, H.-L. Yip, Y. Sun, O. Acton, A. K.-Y. Jen, *Chem. Mater.* **2010**, *22*, 2696; b) G. Zhang, Y. Fu, Q. Zhang, Z. Xie, *Chem. Commun.* **2010**, *46*, 4997; c) Y. Zou, A. Najari, P. Berrouard, S. Beaupré, B. Réda Ai ch, B. Y. Tao, M. Leclerc, *J. Am. Chem. Soc.* **2010**, *132*, 5330; d) C. Piliego, T. W. Holcombe, J. D. Douglas, C. H. Woo, P. M. Beaujuge, J. M. J. Fréchet, *J. Am. Chem. Soc.* **2010**, *132*, 7595.

[9] a) Huo, J. Hou, S. Zhang, H.-Y. Chen, Y. Yang, *Angew. Chem. Int. Ed.* **2010**, *49*, 1500; b) R. Duan, L. Ye, X. Guo, Y. Huang, P. Wang, S. Zhang, J. Zhang, L. Huo, J. Hou, *Macromolecules* **2012**, *45*, 3032.

[10] a) M. H. Chen, J. Hou, Z. Hong, G. Yang, S. Sista, L. M. Chen, Y. Yang, *Adv. Mater.* **2009**, *21*, 4238; b) J. M. Szarko, J. Guo, Y. Liang, B. Lee, B. S. Rolczynski, J. Strzalka, T. Xu, S. Loser, T. J. Marks, L. Yu, L. X. Chen, *Adv. Mater.* **2010**, *22*, 5468; c) S. Subramaniyan, H. Xin, F. S. Kim, S. Shoaee, J. R. Durrant, S. A. Jenekhe, *Adv. Energy Mater.* **2011**, *1*, 854.

[11] a) Y. Y. Liang, Y. Wu, D. Q. Feng, S. T. Tsai, H. J. Son, G. Li, L. P. Yu, *J. Am. Chem. Soc.* **2009**, *131*, 56; b) J. H. Hou, H. Y. Chen, S. Zhang, R. I. Chen, Y. Yang, Y. Wu, G. Li, *J. Am. Chem. Soc.* **2009**, *131*, 15586; c) J. H. Hou, M. H. Park, S. Zhang, Y. Yao, L. M. Chen, J. H. Li, Y. Yang, *Macromolecules* **2008**, *41*, 6012.

[12] Z. Li, S.-W. Tsang, X. Du, L. Scoles, G. Robertson, Y. Zhang, F. Toll, Y. Tao, J. Lu, J. Ding, *Adv. Funct. Mater.* **2011**, *21*, 3331.

[13] a) B. Delley, *J. Chem. Phys.* **1990**, *92*, 508; b) B. Delley, *J. Chem. Phys.* **2000**, *113*, 7756.

[14] V. I. Anisimov, F. Aryasetiawan, A. I. Lichtenstein, *J. Phys.: Condens. Matter* **1997**, *9*, 767.

[15] a) A. D. Becke, *J. Chem. Phys.* **1988**, *88*, 2547; b) C. Lee, W. Yang, R. G. Parr, *Phys. Rev. B* **1988**, *37*, 786.

[16] S. L. Mayo, B. D. Olafson, W. A. Goddard, *J. Phys. Chem.* **1994**, *94*, 8897.

[17] J. K. Lee, W. L. Ma, C. J. Brabec, J. Yuen, J. S. Moon, J. Y. Kim, K. Lee, G. C.Bazan, A. J. Heeger, *J. Am. Chem. Soc.* **2008**, *130*, 3619.

[18] a) R. P. Qin, W. W. Li, C. H. Li, C. Du, C. Veit, H. F. Schleiermacher, M. Andersson, Z. S. Bo, Z. P. Liu, O. Inganas, U. Wuerfel, F. L. Zhang, *J. Am. Chem. Soc.* **2009**, *131*, 14612; b) J. C. Bijleveld, V. S. Gevaerts, D. D. Nuzzo, M. Turbiez, S. G. J. Mathijssen, D. M. de Leeuw, M. M. Wienk, R. A. J. Janssen, *Adv. Mater.* **2010**, *22*, E242.